SWNT GROWTH BY LPCVD ON FERRITIN-BASED IRON CATALYST NANOPARTICLES TOWARDS CNT SENSORS

L. Durrer, T. Helbling, C. Zenger, A. Jungen, C. Stampfer, C. Hierold
Micro and Nanosystems, ETH Zürich, 8092 Zurich, SWITZERLAND
(Tel:+41 44 632 5428; E-mail: lukas.durrer@micro.mavt.ethz.ch)

Abstract: We investigated the growth of individual single-walled carbon nanotubes (SWNTs) by low pressure chemical vapor deposition (LPCVD) on Ferritin-based Fe catalyst. According to Ferritin adsorption measurements, we show that the SWNT density on the surface can be controlled by the Ferritin concentration in the adsorption solution. The grown SWNTs were contacted by Cr/Au layers, structured by electron beam lithography and lift-off, resulting in carbon nanotube (CNT) based field effect transistors (FET).

Keywords: Ferritin adsorption, Fe_2O_3 nanoparticles, SWNT growth, LPCVD, CNT based FET,

1. INTRODUCTION

SWNTs have been shown to act as promising sensing elements in transducers based on FET architecture [1]. However, for the use of SWNTs in batch processes, fundamentals in reproducible growth have to be solved: the control of diameter and chirality, the growth direction and the growth density.

Ferritin-based Fe catalysts are known to yield long SWNTs with narrow diameter distributions and low structural defect densities [2-4]. Ferritin is an iron storage protein, which can upload as many as 4500 iron ions by the oxidation of Fe^{2+} to Fe^{3+}. The iron is stored in the Ferritin body as Ferrihydrite ($5Fe_2O_3 \cdot 9H_2O$) [5]. Because of tedious preparation and lack of surface density control, these catalysts are not common yet.

In this paper, the CNT growth by LPCVD on Ferritin-based Fe particles on 200 nm thick SiO_2 is reported. The influence of the Ferritin iron loading time on the CNT diameter and the influence of the Ferritin adsorption condition on the Ferritin surface density was investigated.

2. EXPERIMENTAL

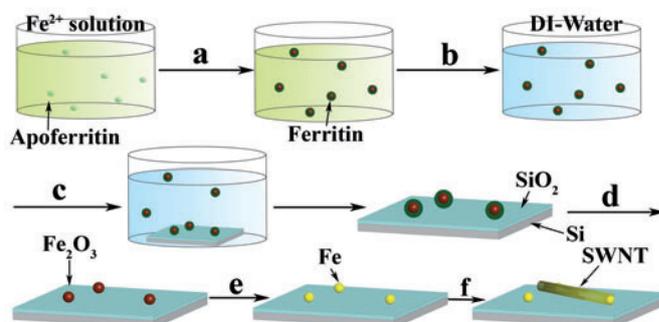Fig. 1 shows the process flow for SWNT-growth on Ferritin-based Fe catalyst. a) Horse spleen

Figure 1: Process flow of SWNT growth by the use of Ferritin-based Fe catalyst: a) Apoferritin loading at 50°C, b) dialysis for 24h and centrifugation for 15min at 14000g, c) Ferritin adsorption on 200nm thick gate oxide, d) oxidation of the organic protein shell at >800°C for 3min, e) reduction of the Fe_2O_3 particles under H_2 atmosphere at 850°C for 10min, f) CNT growth on the freshly formed Fe particles at 800°C and a CH_4/H_2 pressure of 150mbar/50mbar for 15min.

Apoferritin was loaded at 50 °C in a solution containing Fe^{2+}. b) The diluted Ferritin solution was dialyzed against DI-water and centrifuged afterwards. c) The loaded Ferritins were adsorbed on Si/SiO_2. d) The protein shells were oxidized at temperature (T>800 °C). e) In a H_2 pretreatment step, the Fe_2O_3 nanoparticles were reduced. f) CNTs were grown by LPCVD [6].
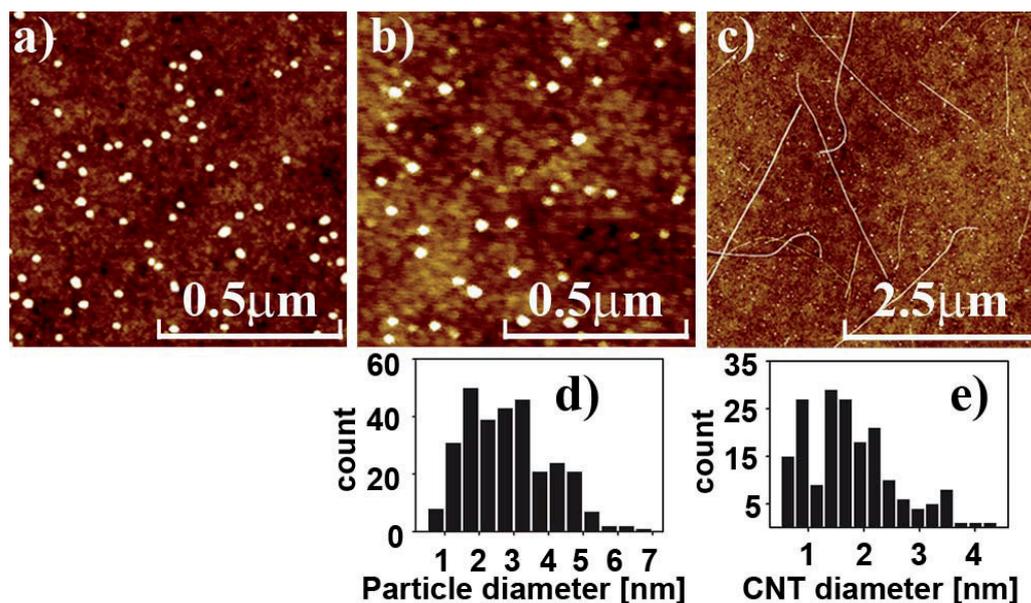
Figure 2: AFM image of a) adsorbed Ferritin, z range: 10nm b) Fe₂O₃ nanoparticles formed by oxidation of the Ferritin shell, z range: 5nm , c) SWNTs grown on the reduced Fe₂O₃ particles, d) diameter distribution histogram of the Fe₂O₃ particles, e) diameter distribution histogram of the grown SWNTs

The contacting of the grown SWNTs by 5 nm Cr and 30 nm Au structured by E-beam and lift-off is described elsewhere [7].

3. RESULTS AND DISCUSSION

Fig. 2a shows an atomic force microscope (AFM) image of a SiO$_2$ surface with Ferritin adsorbed from a 50-times diluted Ferritin solution. The stock solution is commercially available and contains 50-150 mg/ml iron saturated Ferritin. The mean height of the iron loaded proteins is 3.5±1.4 nm and the surface coverage is 70 proteins/µm^2. Fig. 2b shows an AFM image of the resulting Fe$_2$O$_3$ nanoparticles. Fig. 2c shows an AFM tapping mode image of CNTs grown on the Ferritin-based Fe catalyst. In Fig. 2d and 2e, diameter distribution histograms of the formed particles and grown CNTs are shown. The LPCVD process yields CNTs with length between 100 nm and 40 µm. The mean length is 2µm. The CNT density averages measured over 7 AFM images were 0.24±0.21 CNT/particle.

A typical Raman spectrum for SWNTs is shown in Fig. 3. The spectrum was recorded on a surface with CNT grown on Fe particles, yielded from saturated Ferritin proteins. The radial breathing mode (RBM) has a shift of 161 cm^{-1}, from which a SWNT diameter of 1.51 nm can be determined [8]. No D band peak at ca. 130 cm^{-1} mode was obtained, indicating that the SWNT has a very low defect density.

One advantage for the use of Ferritin based iron catalysts for SWNT growth is, that the mean particle diameters can be increased by increasing
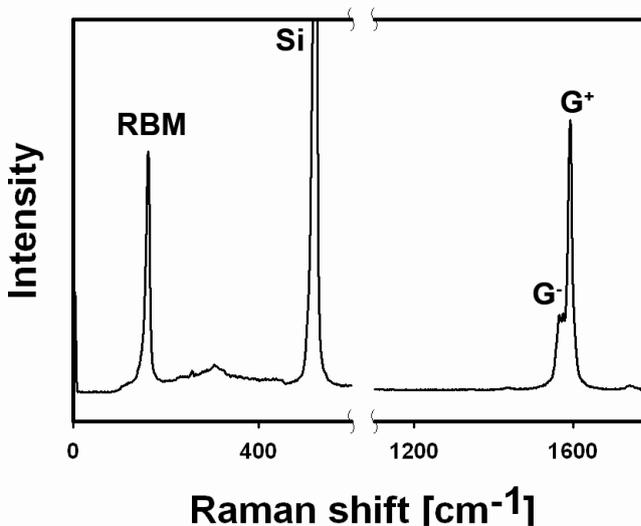

Figure 3: Raman spectrum of a SWNT grown on a Ferritin-based Fe catalyst nanoparticle

188

the Ferritin loading time, which results in an increase of the mean CNT diameter [2]. This is shown in the box plot diagrams of Fig. 4. In Fig. 4a an increase of the median (center line) and the mean (black squared) of the particle diameter by increasing the Ferritin loading time can be seen. In Fig.4b is shown, that the median and the mean of the CNT diameter increases by increasing loading time. The data were obtained from AFM images, as shown in Fig. 2b and 2c. From Fig. 4, it can be concluded, that the particle yield from the self loaded proteins have narrower diameter distributions than particle gained from fully saturated commercially available Ferritin (shaded box plots), resulting in a narrower diameter distribution of the SWNTs.
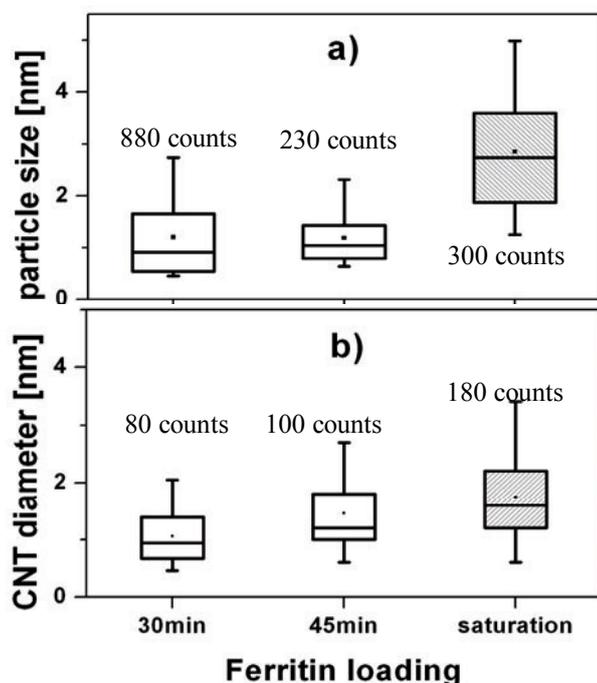

Figure 4: Box plots of a) particle size vs. Ferritin loading b) CNT diameters vs. Ferritin loading

As already mentioned in the introduction, for CNT integration it is important to have control over the CNT density on the surface. In the case of Ferritin based catalyst, the CNT density is proportionally dependent on the Ferritin density on the surface. Fig 5a shows the Ferritin density of adsorbed Ferritin on SiO_2 in dependence of the adsorption time. The density was obtained by AFM tapping mode imaging of a randomly chosen 5x5 μm^2 spot as shown exemplarily in Fig. 2a No significant changes in the Ferritin
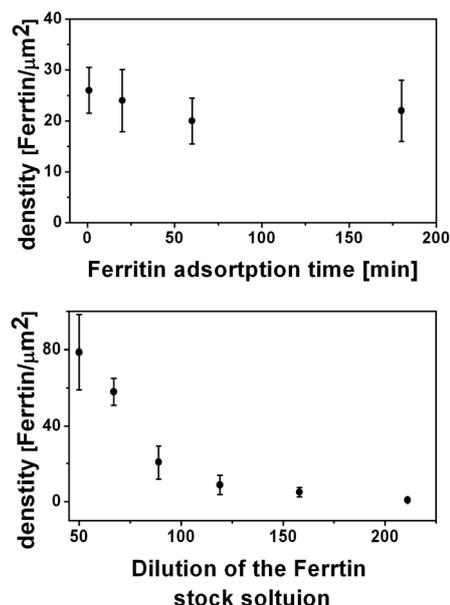

Figure 5: Ferritin density on the SiO_2 surfaces measured by AFM imaging in dependence of a) the Ferritin adsorption time b) the dilution of the Ferritin stock solution

density by increasing the adsorption time were observed. Therefore, the Ferritin adsorption time can be set to 1 min.

Fig. 5b shows the Ferritin density of adsorbed Ferritin on SiO_2 surface in dependence of the dilution of the Ferritin stock solution. Because the Ferritin concentration in the Ferritin stock solution (50-150 mg/ml) is only approximately known, it is not possible to assign the Ferritin concentration quantitatively. This means that for a freshly prepared Ferritin solution, the resulting initial Ferritin density has to be verified. However, the diagram shows that the Ferritin density on the surface decreases by increasing dilution.

Fig. 6 shows an AFM image of an individual SWNT contacted by 4 Cr/Au electrodes. SWNT densities between 0.1 and 0.3 CNTs/μm^2 are desirable for avoiding shorting by other CNTs. To achieve this tube density, a 211 times diluted Ferritin solution of saturated Ferritin was used for Ferritin adsorption. Since SWNTs with several tens of μm were grown, measurements at different places on the same tube can be made.

Fig. 7 shows a typical measurement of a semiconducting SWNT; proving device function. These CNT-based FETs, were used for gas sensor investigation described elsewhere [9].
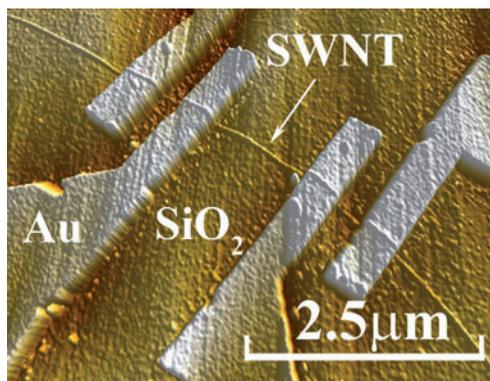
Figure 6: 3D-AFM image of a SWNT grown by LPCVD on Ferritin based Fe catalyst contacted by Cr/Au electrodes structured by E-beam lithography and lift-off, z range: 30nm
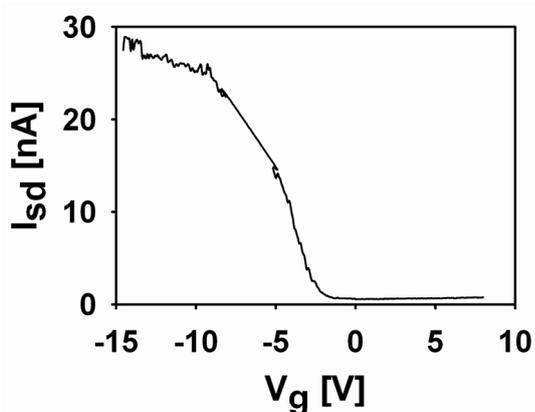

Figure 7: Gate sweep measurement of an integrated semicon-ducting SWNT. The SWNT was grown by LPCVD on a Ferritin-based Fe catalyst. $V_{s\,d}$: 20mV

4. CONCLUSION

SWNTs were grown on Ferritin-based Fe catalyst by LPCVD. In this particular catalyst formation process, Ferritin adsorption investigations led to the control of the SWNT density on the Si/SiO$_2$ surface. This is a step towards controlled CNT integration. However for reproducible CNT devices, the control of the growth direction and of the chirality still has to be investigated.

REFERENCES

[1] N. Sinha, JZ. Ma, JTW. Yeow, "Carbon nanotube-based sensors", J. Nanoscience and Nanotechnology, vol. 6, pp. 573-590, 2006.

[2] YM. Li, W. Kim, YG. Zhang, M. Rolandi, DW. Wang, HJ. Dai, "Growth of single-walled carbon nanotubes from discrete catalytic nanoparticles of various sizes" J. Pys. Chem. B, vol. 105, pp. 11424-11431, 2001.

[3] W. Kim, HC. Choi, M. Shim, YM. Li, DW. Wang, HJ. Dai, "Synthesis of ultralong and high percentage of semiconducting single-walled carbon nanotubes", Nano Letters, vol. 2, pp. 703-708, 2002.

[4] M. Tominaga, A. Ohira, A. Kubo, I. Taniguchi, M. Kunitake, "Growth of carbon nanotubes on a gold(111) surface using two-dimensional iron oxide nano-particle catalysts derived from iron storage protein", Chemical communications vol. 13, pp. 1518-1519, 2004

[5] ND. Chasteen, PM. Harrison, "Mineralization in ferritin: An efficient means of iron storage", Journal of structural biology, vol. 3, pp. 182-194, 1999

[6] A. Jungen, C. Stampfer, L. Durrer, T. Helbling and C. Hierold, "Amorphous carbon contamination monitoring and process optimization for SWNT integration", Nanotechnology, vol. 18, pp. 075603, 2007

[7] C. Stampfer, A. Jungen, C. Hierold, "Fabrication of discrete nanoscaled force sensors based on single-walled carbon nanotubes" IEEE Sensors Journal, vol. 6, pp. 613-617, 2006.

[8] J. Maultzsch, H. Telg, S. Reich, and C. Thomsen, „Radial breathing mode of single-walled carbon nanotubes: Optical transition energies and chiral-index assignment", Physical Review B, vol 72, pp. 205438, 2005

[9] T. Helbling, R. Pohle, C. Stampfer, L. Durrer, A. Goyal, M. Fleischer, C. Hierold, „NO$_2$ Gas Sensor Based on Individual Suspended Single-Walled Carbon Nanotubes", in the Proceedings of the 14th International Conference on solid-State Sensors, Actuators and Microsystems, Lyon, France, June 10-14, 2007